Hindawi
Journal of Advanced Transportation
Volume 2022, Article ID 2087510, 14 pages
https://doi.org/10.1155/2022/2087510

Research Article

Combined Safety and Coordination of Connected Automated Vehicles in Merging Area with Featuring Optimal Merging Positions

Bo Liu[1,2] **Yanqing Cen**,[1] **Zhihong Yao**[3] **Xianghui Song**,[1] **Liu Hongben**[1] **and Huan Gao**[1]

[1]*Research Institute of Highway Ministry of Transport, Beijing 100088, China*
[2]*Department of Automation, Tsinghua University, Beijing 100083, China*
[3]*School of Transportation and Logistics, Southwest Jiaotong University, Chengdu, Sichuan, China*

Correspondence should be addressed to Zhihong Yao; zhyao@swjtu.edu.cn

Received 15 July 2022; Revised 20 August 2022; Accepted 26 August 2022; Published 15 September 2022

Academic Editor: Yang Yang

Freeway on-ramp merging area is deemed to be typical bottlenecks section, which leads to low traffic efficiency, congestions, and frequent accidents. Most existing studies on merging for the connected and automated vehicles focus on merging at a single fixed merging point. However, the problem of coordination between merging vehicle and arterial traffic flow in the acceleration lane is ignored in the existing studies. This study proposes a merging model, which combined safety and coordination of CAVs with featuring optimal merging positions. The proposed model has two stages: one is analysis of merging velocity of the insertable gap and the other one is determining constraint condition of cooperative merging. The outputs of first stage are interval of merging speed and the mergeable range. The outputs of second stage are optional insertable gap and the corresponding driving scheme. Then, a traffic simulation experiment is designed to evaluate the proposed model. The simulation results show that the proposed model can effectively guarantee driving safety and make the merging process smoother with 28.7% reduction in travel time for the CAV merging. Furthermore, the proposed model does not sacrifice the interests of surrounding traffic to assist in CAV merging. The results indicate the promising potential of using the proposed methods can approximately get a fair use of road resources for each CAV.

1. Introduction

The merging area is a typical bottleneck section of the freeway. Most of the problems occur when the on-ramp vehicles merge into the mainline traffic, and in which the low-speed on-ramp vehicles either merge directly or accelerate through the acceleration lane first as well as find a gap for insertion and then search for the opportunity to merge. Because of the interference in space and the large speed differences between on-ramp vehicles and the mainline vehicles, a typical conflict point is formed in the merging area. The conflicts are usually manifested in various traffic events such as on-ramp vehicles stopping to wait and mainline vehicles braking urgently to avoid collisions, which leads to capacity drop, travel delay, increase of fuel consumption and traffic emission, risk of lateral collision, and traffic oscillation [1–3]. Therefore, it is necessary to control and optimize the traffic condition of the merging area.

In the early days, related research generally improved the efficiency and safety of confluence areas from the following two aspects: the first is optimal infrastructure design, by changing the parameters of the infrastructure, such as enlarging the length of the merging section to provide more sufficient space for the on-ramp vehicles and adjusting the merging patterns to reduce conflicts [4–6]. However, the optimization value of infrastructure parameters obtained by such methods is greatly affected by traffic demand, while has a high implementation cost and reconstruction difficulty in

practice, which result in a small scope of application. Therefore, on the premise of the aforementioned method, more study has focused on the second method, which is the control of the balance between on-ramp vehicles merging and mainline vehicles inflow [7–9]. Nonetheless, due to the limitation of traffic flow information perception technology, this kind of model could not respond to the changing traffic flow situation in real time, and the degree of vehicle coordination remains to be further improved.

With the continuous development of wireless communication technology, sensor technology, and automatic driving technology, the emergence of connected and autonomous vehicles (CAVs) and the intelligent roadside unit (RSU) provides an opportunity to improve the merging condition. CAVs are equipped with video detectors, laser radar, and other sensors, which can detect vehicle information within a certain range, such as distance, speed, acceleration, and heading angle. Meanwhile, CAVs also have vehicle-to-X (V2X) communication capability, by which CAVs can share real-time information within the communication range with RSU and other connected vehicles equipped with the on-board unit (OBU) [10–13]. V2X technology contributes to a better awareness of the vehicle motion state and relatively long-range traffic environment, as well as a better information distribution for CAVs.

Therefore, for the connected environment, most of the existing studies rely on V2X technology to carry out merging control for vehicles in the merging area. According to the different control logic, relevant research can be roughly divided into the following two categories: centralized and decentralized [14, 15]. In centralized control, at least one control center is used to globally decide the control strategy of each vehicle. To improve traffic efficiency in merging area, Pueboobpaphan et al. [16] simulated a channel communication algorithm for sending track information to trunk vehicles by a roadside controller. Dan et al. [17] developed an algorithm that combines V2V communication of mainline vehicles with centralized V2I communication to direct ramp vehicles to merge slots. To reduce fuel consumption, Rios Torres et al. designed a centralized merging algorithm through V2I communication to optimize fuel consumption and it was shown to reduce fuel consumption by 49.8% [18]. Min et al. [19] focused on the scenario of CAVs on-ramp merging and proposed a centralized control method to solve the problems of merging sequence (MS) allocation and motion planning. However, the computation and communication cost of the centralized approach becomes larger as the number of vehicles to be controlled increases, leading to the excessive delay of the control policy and the failure of meeting the requirements of real-time dynamic planning. Besides, the limited infrastructure such as the control center may be a burden as the control area expands.

Conversely, in decentralized control, each individual vehicle obtains information based on the V2X communication with adjacent OBU and RSU and develops its own control strategy. Due to the loss of the control center limit, compared with centralized control, decentralized control has low implementation cost, relatively low delay, and good scalability, which is widely used in multivehicle control [20–22]. However, the cooperative merging model based on the decentralized control also exists research challenges. (1) First, as for the setting of the merging point, some of the current models require on-ramp vehicles to merge at a single fixed merging point [23, 24]. For example, Xiao et al. [25] brought together control barrier functions (CBFs), control Lyapunov functions (CLFs), and optimal control to provide an efficient solution to the merging problem in traffic networks. But this approach is developed in the scenario where CAVs randomly arrive at the mainline and the ramp respectively and then cross the fixed merging point in their arrival order, obeying the principle of "first-in-first-out". Obviously, the stationary merging position fails to make full advantage of the space resource of the merging section, bringing the potential negative effects of congestion when expanded to some other traffic rates. (2) Second, existing studies usually concentrate on the complete connected environment [26–29]. Scholte et al. proposed a control strategy for the merging of a single vehicle into a cooperative platoon [30]. Although it is more convenient to build cooperative rules and merging models, quite some time is still required to achieve above conditions. At present, to study mixed traffic flow scenarios can be of more practical significance and application value. (3) Third, most of the cooperative and decentralized methods focus on the optimization of traffic flows in merging areas that are composed of single-lane freeways. Tianyi [31] proposed a rotation-based CAV distributed cooperative control strategy for an on-ramp merging scenario where the mainline and ramp line are single and straight. Sun et al. (2020) [32] studied cooperative decision-making for mixed traffic by assuming an idealistic ramp-merging section has a single lane at the mainline and an on-ramp lane. Furthermore, the synergistic mechanism between lane-changing behavior of upstream vehicles on mainline and on-ramp vehicle merging strategy should also be further studied.

To sum up, this study provides contributions to CAV merging in the following directions: (i) the merging point is dynamically determined based on the coordination with the arterial traffic as shown in Section 2.3. Different from the fixed merging point, through the dynamic analysis of the arterial traffic flow, the optimal merging position is reasonably determined for each CAV under the current situation. This method can ensure the safety of merging and give the dynamic merging position to make full use of the space resources of the acceleration lane. (ii) The proposed model, which considers both safety and efficiency, only requires infrastructure-vehicle communication. Different from the existing researches, the proposed model does not rely on vehicle-vehicle communication. According to vehicle-infrastructure communication and the prediction mechanism considering communication delay, the secure merging strategy of CAV can be effectively given. The proposed model is suitable for mixed traffic flow because it does not rely on vehicle-vehicle communication with full coverage.

The input information of the proposed model includes arterial traffic flow information collected by roadside sensors, vehicle-infrastructure communication information, etc. The vehicle types covered include human-driven vehicles (which can be mixed traffic) for the arterial and the

merging CAV. Therefore, this study involves the coordinated control of human-driven vehicles and CAVs as well as the dynamic response of the communication between roadside sensors and infrastructure-vehicle communication. The remainder of the study is organized as follows: in Section 2, we introduce the merging velocity analysis model and the constraint condition of cooperative merging. In Section 3, the detailed experimental design is given based on the traffic simulation. Section 4 presents and discusses the results of the experimental design from different analysis perspectives. Finally, Section 5 concludes the study with future work directions.

2. Method

2.1. Model Assumptions. To solve the problem of safe and efficiency merging of vehicles in merging area, an analysis model of merging velocity and cooperative merging is proposed. To derive the merging strategy for a series of vehicles arrived in succession, the following assumptions are made:

(1) In merging area, the vehicles of arterial traffic will not change lanes unless necessary.

(2) In merging area, the vehicles of arterial traffic will not change driving behavior. In other words, if the vehicle has a constant speed before entering the merging area, it will remain moving at this constant speed after entering.

(3) When a vehicle travels in a straight line, it is approximately parallel to the longitudinal direction, so the heading angle is 0.

(4) In this study, no specific lane change track analysis is made, only the lane change safety is constrained, and the lane change time is uniformly fixed.

(5) By default, all vehicles have the same level of motion performance. That is, the max acceleration and the max deceleration are the same.

(6) In the acceleration lane area, in order to ensure the safety of the rear vehicles, any deceleration behavior of the CAV does not be considered when it is not necessary.

2.2. Analysis of Merging Velocity of the Insertable Gap. In merging area of freeway, the vehicles need to accelerate to a reasonable speed through the acceleration lane area so that they can safely and efficiently merge into the arterial traffic, as shown in Figure 1.

The acceleration lane starts at point C and ends at point E. The length of acceleration lane is L^{al}. The speed limit in the acceleration lane $v_{\max}^{al}$ is 100 km/h. According to the vehicle position data from the detector of roadside infrastructure (like lidar, camera) or on-board unit (OBU) of vehicle, we can identify the position of the incoming vehicle C_1 that is about to enter the acceleration lane area (about to reach point C). The vehicle C_1 is the object for which the proposed model will provide the auxiliary merging strategy.

Due to the max speed limit of the acceleration lane, the vehicle does not chase the far ahead insertable gap at excessive acceleration. Moreover, the speed of on-ramp vehicles is generally lower than the target lane of the arterial. When the vehicle C_1 reaches point C, only vehicles in the range $[x_{C_1}^{al,c}, x_{C_1}^{al,c} + L^{al}/2]$ ahead are considered. The vehicle most in front of vehicle C_1 in this range is denoted as D_1, and the vehicle behind the arterial is denoted as D_{n+1} in turn where $n \geq 2$ and $n \in \mathrm{N}$. According to the model assumption (6), vehicles do not slow down when it is not necessary. Therefore, the running time of vehicle C_1 in the acceleration lane is less than $L^{al}/v_{\min}^{al}$. $v_{\min}^{al}$ is the min speed of the vehicle in the acceleration lane, generally 40 km/h. Because it is a highway, there is a min speed limit $v_{\min}^{tl}$ in the target lane of the arterial. When vehicle C_1 reaches point C, it only needs to consider the insertable gap within the rear range $[x_{C_1}^{al,c} - v_{\min}^{tl} \cdot (L^{al}/v_{\min}^{al}), x_{C_1}^{al,c}]$. To sum up, vehicle C_1 only needs to consider the insertable gap within range $[x_{C_1}^{al,c} - v_{\min}^{tl} \cdot (L^{al}/v_{\min}^{al}), x_{C_1}^{al,c} + (L^{al}/2)]$ of the target lane.

It is worth noting that the vehicle position information in the target lane is mainly sensed through the roadside detector. However, the roadside detector sends the arterial traffic information (vehicle position, speed, acceleration, gap, etc.) to the incoming vehicle of the acceleration lane at t_0. Considering the inevitable communication delay τ exists in the I2V (infrastructure to vehicle) communication process, the incoming vehicle actually receives the information at t_1, namely, $\tau = t_1 - t_0$. Since the vehicle speed on the arterial is faster and the gap between two vehicles is smaller, the influence of communication delay on the gap change of two vehicles needs to be considered. For merging safety, the length of the insertable gap is the smallest possible value in the proposed model. In the communication delay τ, the displacement of the preceding vehicle in the target lane:

$$x_n = \frac{1}{2} a_{D_n}(t_0) \cdot \tau^2 + \frac{1}{3.6} v_{D_n}(t_0) \cdot \tau. \tag{1}$$

The displacement of the following vehicle is calculated as follows:

$$x_{n+1} = \frac{1}{2} a_{D_{n+1}}(t_0) \cdot \tau^2 + \frac{1}{3.6} v_{D_{n+1}}(t_0) \cdot \tau, \tag{2}$$

where $v_{D_n}(t_0)$ is the speed of vehicle D_n in the target lane at time t_0 and the unit is km/h. $a_{D_n}(t_0)$ is the acceleration of vehicle D_n and the unit is m/s^2. x_n is the position of vehicle D_n at the longitudinal direction. The displacement between two vehicles during τ is calculated as follows:

$$\Delta x = x_{n+1} - x_n. \tag{3}$$

Due to the volatility of communication delay (delay is generally τ, but may be 0 sometimes), the gap change under the influence of delay is only considered as the minimum value to avoid wrong estimation. If $\Delta x < 0$, the gap gap_n is smaller than that of t_0. The min possible value of the gap gap_n' is shown in the following formula at time t_1:

$$\mathrm{gap}_n' = \mathrm{gap}_n + \Delta x \tag{4}$$

If $\Delta x \geq 0$, the gap gap_n is bigger than that of t_0. The min possible value of the gap gap_n' is shown in the following formula at time t_1:

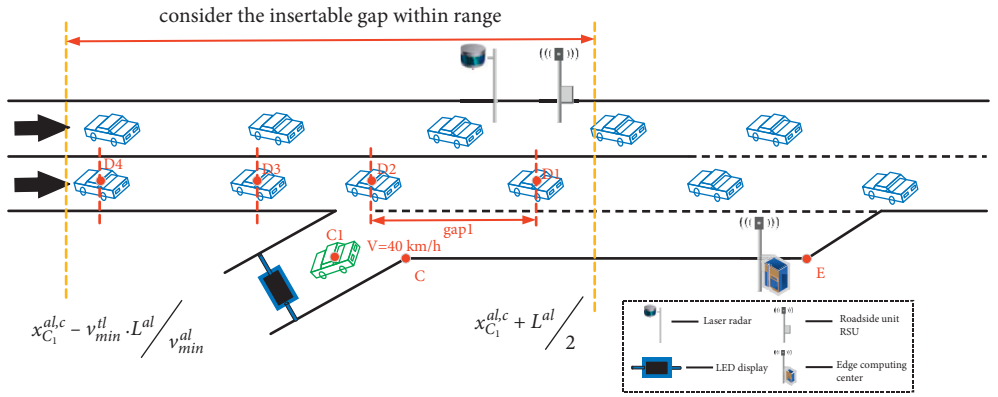

Figure 1: The scene of CAVs in the merging area.

$$\text{gap}_n' = \text{gap}_n \tag{5}$$

In this study, the specific lane change trajectory is not considered, but the lane change safety constraints are considered for the merging process. During lane change, the change of lateral velocity is independent of the change of longitudinal velocity. As shown in Figure 2, during lane change, the longitudinal distance $S_{i,j}(t)$ between the merging vehicle C_i and the preceding vehicle D_j in the target lane is expressed as follows:

$$S_{i,j}(t) = x_j(t) - x_i(t) - W_i \cdot \sin(ha(t)), \tag{6}$$

where $x_j(t)$ and $x_i(t)$ are, respectively, the positions of the merging vehicle and the preceding vehicle in the target lane at time t. W_i is the width of the vehicle. Heading angle ha is defined as included angle between the tangent direction of vehicle trajectory and the longitudinal of the lane boundary and there is the following formula:

$$\begin{aligned}\tan(ha(t)) &= \frac{\partial y_{C_i}(t)}{\partial x_{C_i}(t)} \\ &= \frac{\partial y_{C_i}(t)/\partial t}{\partial x_{C_i}(t)/\partial t} \\ &= \frac{v_{C_i}^{\text{lat}}(t)}{v_{C_i}(t)}.\end{aligned} \tag{7}$$

If $S_{i,j}(t) > 0, \quad t \in [t_0, t_{\text{end}}]$, it can ensure that there is no collision between the merging vehicle and the preceding vehicle in the target lane during the whole lane change period. Combined with vehicle kinematics, the safety constraint expression can be transformed into the following formula. Such detailed analysis can be seen in Hossein et al., Yang et al., and Alexander et al. [32–35], and this study does not do theoretical derivation (Figure 2):

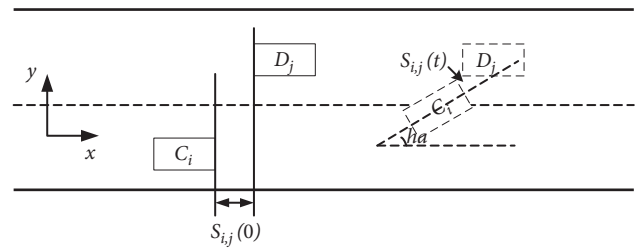

Figure 2: The lane change safety constraint from the preceding vehicle.

$$\begin{aligned}S_{i,j}(t) = {} & S_{i,j}(t_0) - W_{C_i} \cdot \sin(ha(t)) \\ & + \iint_{t=t_0} \left(a_{D_j} - a_{C_i} \cdot \cos(ha(t))\right) dt \\ & + \left(v_{D_j}(t_0) - v_{C_i}(t_0)\right) \cdot t.\end{aligned} \tag{8}$$

In the merging process, the heading angle ha is not too big and the width of the vehicle is generally less than 1.6 m. Hence, the value of $W_{C_i} \cdot \sin(ha(t))$ is negligible. The merging vehicle trajectories are not considered in this study. To simplify the model, four equations are defined in this study:

$$\begin{aligned}& f_{pv}^{a}\left(D_j, C_i, ha(t), t\right) \\ & \quad = \iint_{t=t_0} \left(a_{D_j} - a_{C_i} \cdot \cos(ha(t))\right) dt, \\ & f_{pv}^{v}\left(D_j, C_i, t\right) = \left(v_{D_j}(t_0) - v_{C_i}(t_0)\right) \cdot t, \\ & f_{fv}^{a}\left(C_i, D_{j+1}, ha(t), t\right) \\ & \quad = \iint_{t=t_0} \left(a_{C_i} \cdot \cos(ha(t)) - a_{D_{j+1}}\right) dt, \\ & f_{fv}^{v}\left(C_i, D_{j+1}, t\right) = \left(v_{C_i}(t_0) - v_{D_{j+1}}(t_0)\right) \cdot t.\end{aligned} \tag{9}$$

As shown in Figure 3, the headway $h_{C_1,D_n}(t)$ between the merging vehicle C_1 and the preceding vehicle D_n in the target lane should be satisfied:

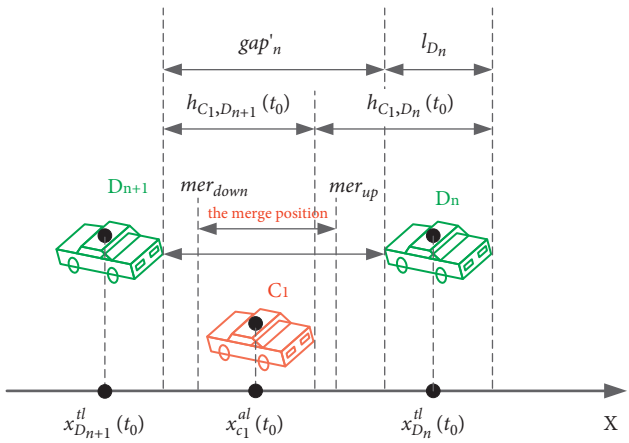

Figure 3: Relation of the gap and headway.

$$h_{C_1,D_n}(t) = h_{C_1,D_n}(t_0) - l_{D_n} + f^a_{pv}(D_n, C_1, ha(t), t) + f^v_{pv}(D_n, C_1, t), \quad h_{C_1,D_n}(t) > 0, \quad t \in [t_0, t_{\text{end}}]. \tag{10}$$

Under the security constraint, if $h_{C_1,D_n}(t)$ is non-negative at time $t = t_0$, it can be guaranteed to be non-negative at $t \in [t_0, t_{\text{end}}]$. Due to the model assumption (3), $\cos(ha(t_0)) = 1$. That is to say, the collision avoidance condition is as follows:

$$h_{C_1,D_n}(t_0) - l_{D_n} + f^a_{pv}(D_n, C_1, ha(t_0), t_0) + f^v_{pv}(D_n, C_1, t_0) > 0. \tag{11}$$

In the same way, the collision avoidance condition between the merging vehicle C_1 and the following vehicle D_{n+1} in the target lane is as follows:

$$h_{C_1,D_{n+1}}(t_0) - l_{C_1} + f^a_{fv}(C_1, D_{n+1}, ha(t_0), t_0) + f^v_{fv}(C_1, D_{n+1}, t_0) > 0. \tag{12}$$

To sum up, considering the impact of communication delay τ, the determination conditions of insertable gap are as follows:

$$\begin{cases} h_{C_1,D_n}(t_0) - l_{D_n} + f^a_{pv}(D_n, C_1, ha(t_0), t_0) + f^v_{pv}(D_n, C_1, t_0) > 0, \\ h_{C_1,D_{n+1}}(t_0) - l_{C_1} + f^a_{fv}(C_1, D_{n+1}, ha(t_0), t_0) + f^v_{fv}(C_1, D_{n+1}, t_0) > 0, \\ h_{C_1,D_n}(t_0) + h_{C_1,D_{n+1}}(t_0) - l_{D_n} \le \text{gap}'_n. \end{cases} \tag{13}$$

By solving the previous formula, the corresponding interval of merging speed of the insertable gap can be obtained, represented by $(v_{\text{down}}, v_{\text{up}})$. According to the relation of headway, the relative position of vehicles in the gap when merging is obtained, that is, the requirement of the merge position $(\text{mer}_{\text{down}}, \text{mer}_{\text{up}})$. It is important to note that mer_{down} and mer_{up} are relative positional representations of gap, as shown in Figure 4(b). The merge position can be calculated based on $h_{C_1,D_n}(t)$, $h_{C_1,D_{n+1}}(t)$ and the location of FV or PV of the target lane.

2.3. Constraint Condition of Cooperative Merging. Considering the length limit of the acceleration lane and the performance of the vehicle itself (mainly the maximum acceleration), it may not be able to accelerate to the merging speed v_{mer} (v_{mer} is the median value of the interval $(v_{\text{down}}, v_{\text{up}})$) and drive to the corresponding merging position in the acceleration lane. Therefore, it is necessary to judge that the vehicle can meet the merging speed and position requirements of the target insertable gap by combining the limiting conditions. There are two levels of judgment: one level, the vehicle C_1 to be merged in the acceleration lane accelerates to the merging speed of the target insertable gap at the max acceleration $a_{\max}$; the other level, after the acceleration, the proposed model is discussed in terms of the relationship between the position of vehicle C_1 and the insertable gap. There are three types of situations after the vehicle C_1 accelerates to v_{mer}.

Situation 1. The merging vehicle is behind the insertable gap.

When the merging vehicle C_1 accelerates to v_{mer}, it is behind the insertable gap. In this situation, there are two cases (the relation between merging speed v_{mer} and the speed of the following vehicle $v_{D_{n+1}}$ in the target lane).

Case 1. If $v_{\text{mer}} \le v_{D_{n+1}}$, the vehicle C_1 cannot be merged into the insertable gap. The driving strategy for the merging vehicle C_1 to accelerate to v_{mer} with the max acceleration $a_{\max}$ is the fastest approach to the target gap'_n. If the vehicle C_1 does not catch up with the following vehicle D_{n+1} after the completion of acceleration, and the current speed of the vehicle C_1 is lower than the vehicle D_{n+1}, the distance between the merging vehicle and the target insertable gap will continue to increase, resulting in the failure to complete the merging.

Case 2. If $v_{\text{mer}} > v_{D_{n+1}}$, the vehicle C_1 can be merged into the insertable gap under certain constraints. Although the vehicle C_1 is located behind the gap after completing acceleration, since the speed of the vehicle C_1 is higher than the following vehicle D_{n+1}, the vehicle C_1 may overtake the vehicle D_{n+1} after driving at constant speed v_{mer} for a period of time to reach the merge position and complete merging. Considering the length limit of the acceleration lane, the vehicle C_1 must meet the following conditions:

$$\% \begin{cases} \int\int_{t_0}^{t_1} a^{al}_{C_1}(t)dt + v_{\text{mer}} \cdot (t - t_1) \le L^{al}, \\ v_{D_{n+1}} \cdot t + \text{mer}_{\text{down}} \le x^{al,c}_{C_1} \\ + \int\int_{t_0}^{t_1} a^{al}_{C_1}(t)dt + v_{\text{mer}} \cdot (t - t_1) \le v_{D_{n+1}} \cdot t + \text{mer}_{\text{up}}. \end{cases} \tag{14}$$

Here, $a^{al}_{C_1}(t) = \begin{cases} a_{\max}, & t_0 \le t < t_1 \\ 0, & t > t_1 \end{cases}$.

Situation 2. The merging vehicle is in the insertable gap.

In this situation, according to the relative position of the vehicle C_1 in the gap'_n and the merged interval $(\text{mer}_{\text{down}}, \text{mer}_{\text{up}})$, it can be divided into two subsituations.

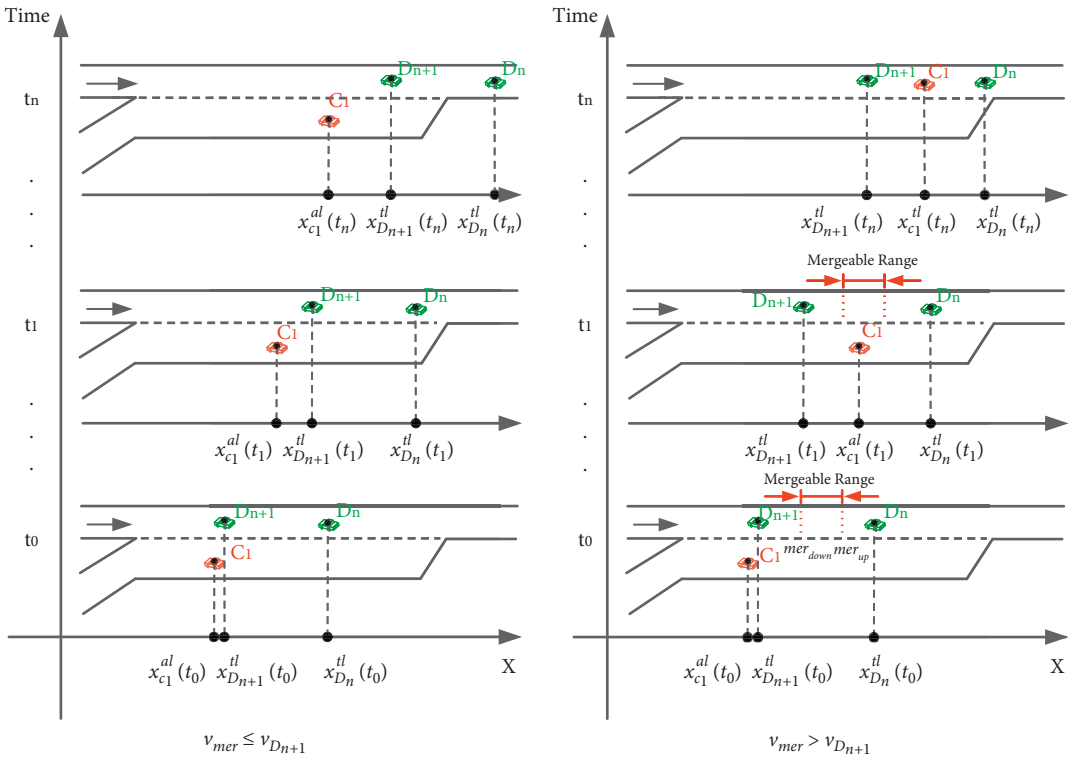

Figure 4: The merging vehicle is behind the insertable gap.

Subsituation 1. The vehicle C_1 is behind the merged interval $(\text{mer}_{\text{down}}, \text{mer}_{\text{up}})$. There are two cases as shown in Figure 5.

Case 3. If $v_{\text{mer}} \le v_{D_{n+1}}$, the vehicle C_1 cannot be merged into the insertable gap. This case is similar to situation 1-Case 3.

Case 4. If $v_{\text{mer}} > v_{D_{n+1}}$, the vehicle C_1 can be merged into the insertable gap under certain constraints. This case is similar to situation 1-Case 4. The merging conditions are similar to equation (14), except for the size of constant running time t.

Subsituation 2. The vehicle C_1 is in front of the merged interval $(\text{mer}_{\text{down}}, \text{mer}_{\text{up}})$. There are two cases as shown in Figure 6.

Case 5. If $v_{\text{mer}} \le v_{D_{n+1}}$, the vehicle C_1 can be merged into the insertable gap under certain constraints. The vehicle C_1 is located in the gap after completing acceleration, but it has exceeded the merging position during acceleration. As the speed of the vehicle C_1 is less than the vehicle D_{n+1}, it is possible for the vehicle C_1 to reach the merging position and complete the merging after running at constant speed v_{mer} for a period of time. The merging conditions are similar to equation (14).

Case 6. If $v_{\text{mer}} > v_{D_{n+1}}$, the vehicle C_1 must be merged into the insertable gap under certain constraints. The vehicle C_1 is located in the gap after completing acceleration, but it has exceeded the merging position during acceleration. As the speed of the vehicle C_1 is bigger than the vehicle D_{n+1}, running at constant speed v_{mer} cannot meet the merging. Therefore, if the acceleration is uniformly accelerated with an acceleration lower than $a_{\max}$ in the acceleration process, the acceleration to v_{mer} will be appropriately slowed down and the timing of merging will be delayed. The merging conditions are as follows:

$$\begin{cases} \int\int_{t_0}^{t} a_{C_1}^{al}(t)dt + v_{C_1}^{al} \cdot t \le L^{al}, \\ v_{D_{n+1}} \cdot t + \text{mer}_{\text{down}} \le x_{C_1}^{al,c} \\ + \int\int_{t_0}^{t} a_{C_1}^{al}(t)dt + v_{C_1}^{al} \cdot t \le v_{D_{n+1}} \cdot t + \text{mer}_{\text{up}}. \end{cases} \tag{15}$$

Situation 3. The merging vehicle is in front of the insertable gap.

In this situation, there are two cases as shown in Figure 7.

Case 7. If $v_{\text{mer}} \le v_{D_{n+1}}$, the vehicle C_1 can be merged into the insertable gap under certain constraints. This case is similar to situation 2-subsituation 2-Case 7. The merging conditions are similar to equation (14).

Case 8. If $v_{\text{mer}} > v_{D_{n+1}}$, the vehicle C_1 must be merged into the insertable gap under certain constraints. This case is similar to situation 2-subsituation 2-Case 8. The merging conditions are similar to equation (15).

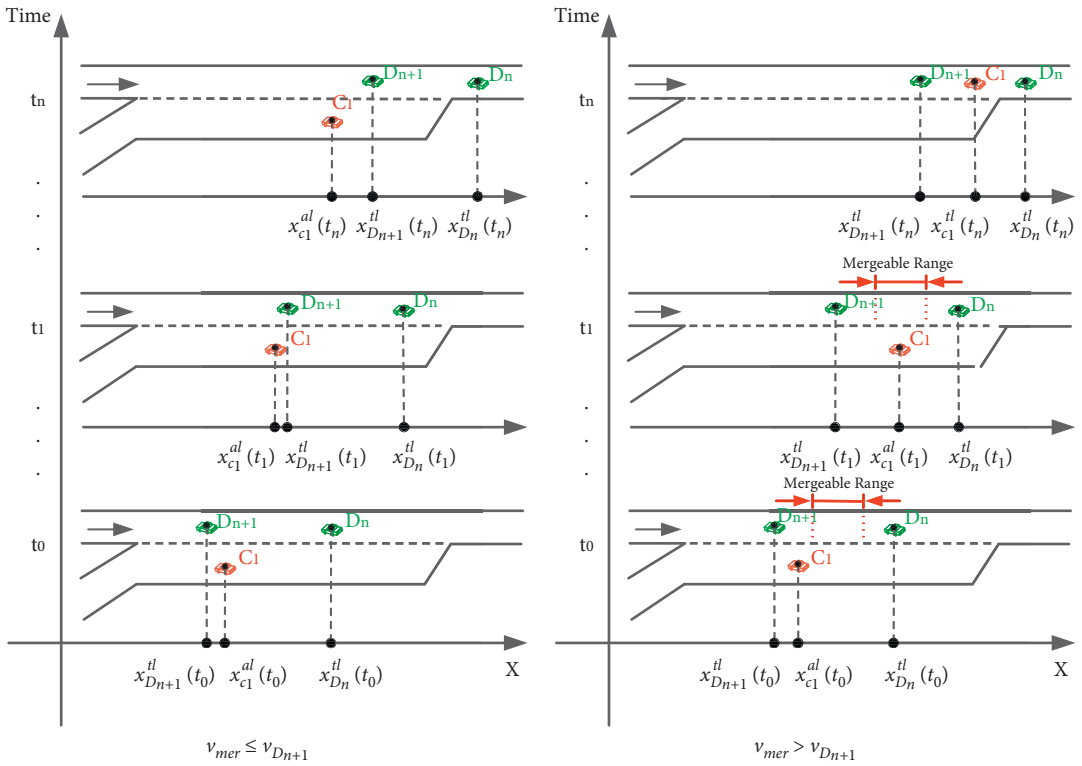

Figure 5: The merging vehicle is behind the merged interval.

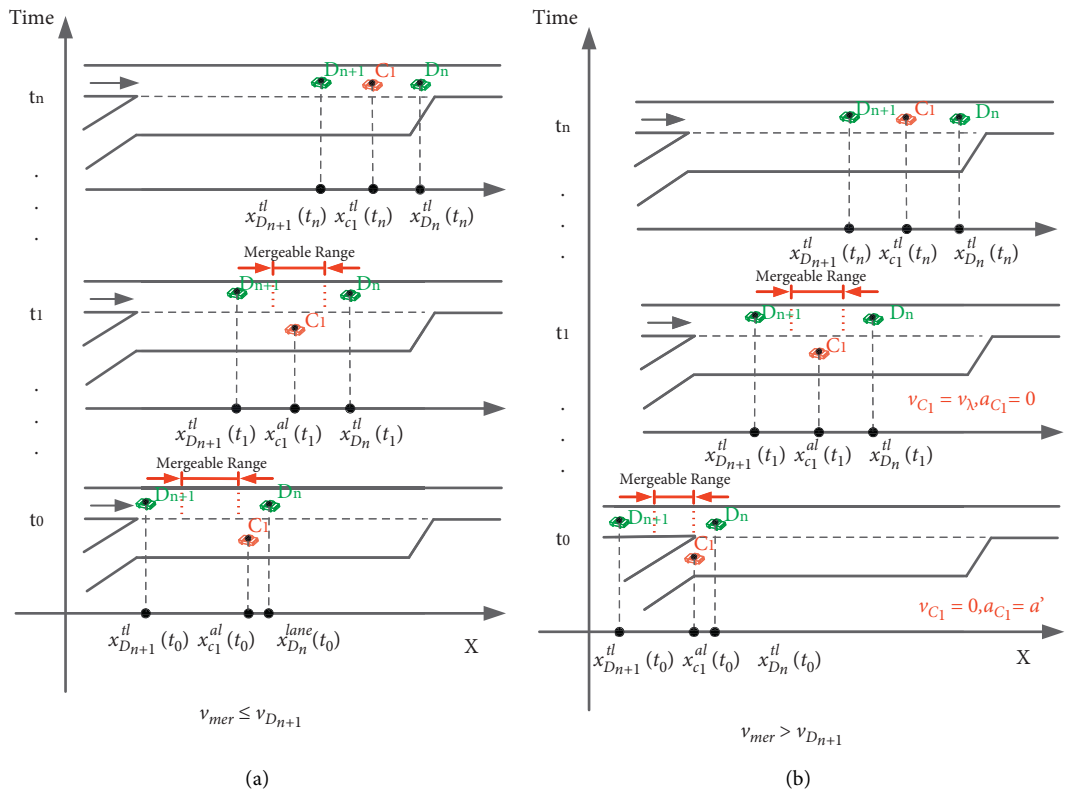

Figure 6: The merging vehicle is in front of the merged interval.

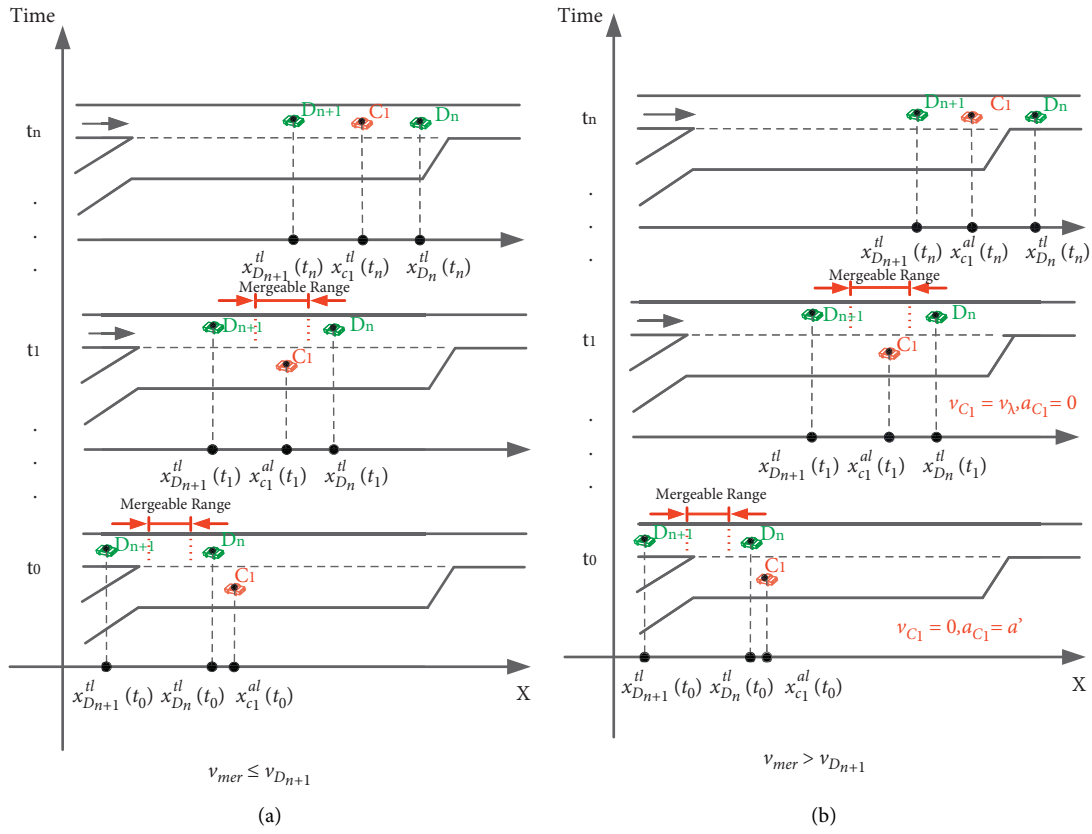

Figure 7: The merging vehicle is in front of the insertable gap.

To sum up, based on the insertable gap obtained by Section 2.2 and the requirements of merging speed and position, Section 2.3 completes the judgment of whether the vehicle can merge into the target insertable gap. The implementation algorithm of the proposed model is listed in Table 1. The finally obtained insertable gap may not be unique. Since the proposed model focuses on the safety of merging vehicles, a feasible solution can be selected in the end. Therefore, the first insertable gap satisfying the conditions is selected as the final insertable gap.

3. Experimental Design

To evaluate the proposed algorithm, a case study was conducted. The case study utilized traffic simulation data. The simulation environment was built with MATLAB, as shown in Figure 8. In the case study, we set the arterial into three lanes and take the center line of the second lane as the X-axis, with the forward direction as the traffic direction.

Due north is the positive Y direction. The angle between the on-ramp and the arterial is θ and $\tan(\theta) = 1/6$. The acceleration lane starts at 925 m and ends at 1125 m, with a total length of 200 m.

In the arterial, the total traffic flow of three lanes is 3000 veh/h, and human driven vehicles are randomly generated in each lane according to Poisson distribution. The length of the vehicles is 4.3 m and the width is 1.8 m. In the on-ramp lane, we generated 6 CAVs at fixed interval 6 s between 70 s and 106 s. The total simulation time is 200 s. Based on the model assumption (1), only the following model needs to be considered and human driven vehicles using IDM (intelligent driver model) model and CAVs using the ACC (adaptive cruise control) model. Specific parameters are described as follows.

For IDM model, the desired acceleration and deceleration are 5 m/s^2 and -5 m/s^2, respectively. The safe headway is 1.8 s. The desired speed is 30 m/s. The minimum distance at a standstill is 5 m.

For ACC model, the minimum distance at a standstill is 5 m. The comfortable acceleration is 3 m/s^2. The max speed is 120/3.6 m/s. The max acceleration and deceleration are 5 m/s^2 and -8 m/s^2, respectively. The response time is 0.1 s. The control parameters are $k_1 = 0.45$ and $k_2 = 0.25$.

In the initial network, after the arterial traffic flow is generated according to Poisson distribution, the time of traffic flow generation and random initial speed are recorded to form the arterial data set U_{art}. The experiment is divided into two stages.

Stage 1. At the beginning of the experimental simulation, the data set U_{art} was loaded to simulate the operation of the traffic flow in the merging area in normal mode (merging traffic flow was not guided), and the speed, acceleration, and position data of all vehicles (arterial traffic flow and merging traffic flow) at the whole time in the merging area were recorded as "normal merging."

Table 1: The implementation algorithm of the proposed model.

Algorithm
1. Initializing the Network ① IDM parameters setting $\mathbf{S} = 5\mathbf{m}$, $\mathbf{Tsaf} = 1.8\mathbf{s}$, $\mathbf{a_{max}} = 5\mathbf{m/s^2}$, $\mathbf{b_{max}} = -5\mathbf{m/s^2}$ ② ACC parameters setting $\mathbf{S} = 5\mathbf{m}$, $\mathbf{Tsaf} = 1.1\mathbf{s}$, $\mathbf{a_{max}} = 5\mathbf{m/s^2}$, $\mathbf{b_{max}} = -8\mathbf{m/s^2}$, $\mathbf{k}_1 = 0.45$, $\mathbf{k}_2 = 0.25$ ③ Vehicles generating Volume ← 3000 **veh/h** Statistical characteristics of traffic flow ← Poisson distribution On-ramp area ← $900\mathbf{m} - 1150\mathbf{m}$ ④ Simulation time setting $\mathbf{t} = 2000\mathbf{s}$, step size ← $\mathbf{dt} = 0.1\mathbf{s}$ Starting simulation: $\mathbf{t} = 0\mathbf{s}$, go to step 2.
2. Calculate the range of the insertable gap: $[x_{C_1}^{al,c} - v_{\min}^{tl} \cdot (L^{al}/v_{\min}^{al}), x_{C_1}^{al,c} + (L^{al}/2)]$, go to step 3.
3. ① Calculate the min possible value of the gap $\mathbf{gap_n'}$ ② Put all $\mathbf{gap_n'}$ in the set $\mathbf{G} = \{\mathbf{gap_n'}\}$, go to step 4.
4. ① Set n = 1 ② Take $\mathbf{gap_n'}$ from G and get $\mathbf{v_{D_n}}$, $\mathbf{v_{D_{n+1}}}$, go to step 5.
5. ① Calculate the merging speed $(\mathbf{v_{do\ wn}}, \mathbf{v_{up}})$ and get the median value $\mathbf{v_{mer}}$ ② Calculate the merging position $(\mathbf{mer_{do\ wn}}, \mathbf{mer_{up}})$ ③ Compare $\mathbf{x_{C_1}}$ and the position of $\mathbf{gap_n'}$ ⟶ Choose *'Situation'* ④ Compare $\mathbf{x_{C_1}}$ and $(\mathbf{mer_{do\ wn}}, \mathbf{mer_{up}})$ ⟶ Choose *'Sub-situation'* ⑤ Compare $\mathbf{v_{mer}}$ and $\mathbf{v_{D_{n+1}}}$ ⟶ Choose *'Case'*, go to step 6.
6. ① Calculate and analyze driving scheme ⟶ Based on (14) and (15) ② If there's a solution, end; otherwise, set n = n+1, go to step 4-②.

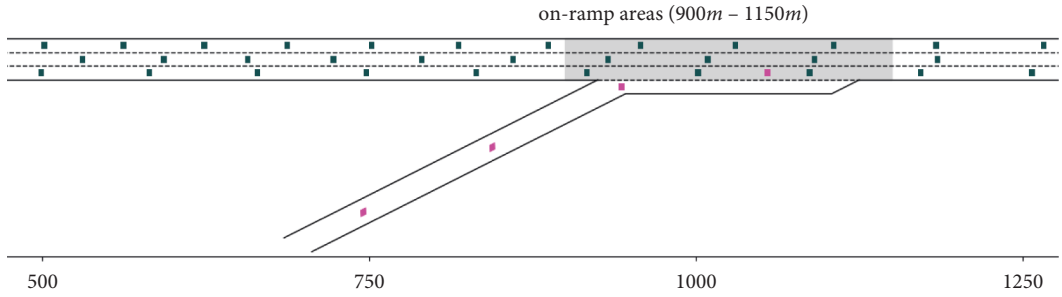

Figure 8: Traffic simulation data collection network.

Stage 2. Clear the simulation environment and reload data set U_{art}. The proposed model is applied to merging traffic flow. In the same way, the speed, acceleration, and position data of all vehicles at the whole time in the merging area were recorded as the "proposed model." Compare the difference between "normal merging" and "proposed model" to analyze the superiority of the proposed model.

4. Result Analysis

Due to the experimental design of Section 3, we eliminated the interference (random loading of traffic flow results in the inconsistent traffic flow of each simulation) of arterial traffic flow, on-ramp traffic flow, and so on. As shown in Figure 9, the curve of the speed, acceleration, and position is drawn, where the solid blue line is the merging CAV vehicle, the yellow dotted line is the following vehicle of the target lane and the pink dotted line is the preceding vehicle of the target lane. Each row in Figure 9 represents the data of a merging CAV.

By observing the velocity curve (column 1) and the position curve (column 3), it can be found that there are phases where the velocity is zero (like on-ramp 12 CAV and on-ramp 21 CAV) and phases where the position is constant (like on-ramp 12 CAV and on-ramp 21 CAV). It indicates that CAV3 and CAV6 stopped in the acceleration lane. It should be noted that "12" in the legend represents the vehicle number in the target lane after CAV3 merges the target lane. IDM 13-FV and IDM 11-PV are the following vehicle and the preceding vehicle of the target lane, respectively.

From the position curve, CAV2, CAV4, and CAV5 seem to have stopped, but by observing the velocity curve, there is no case that the velocity is 0 in a period of time. This is because at low speed, the travel distance in a short time is smaller, and the

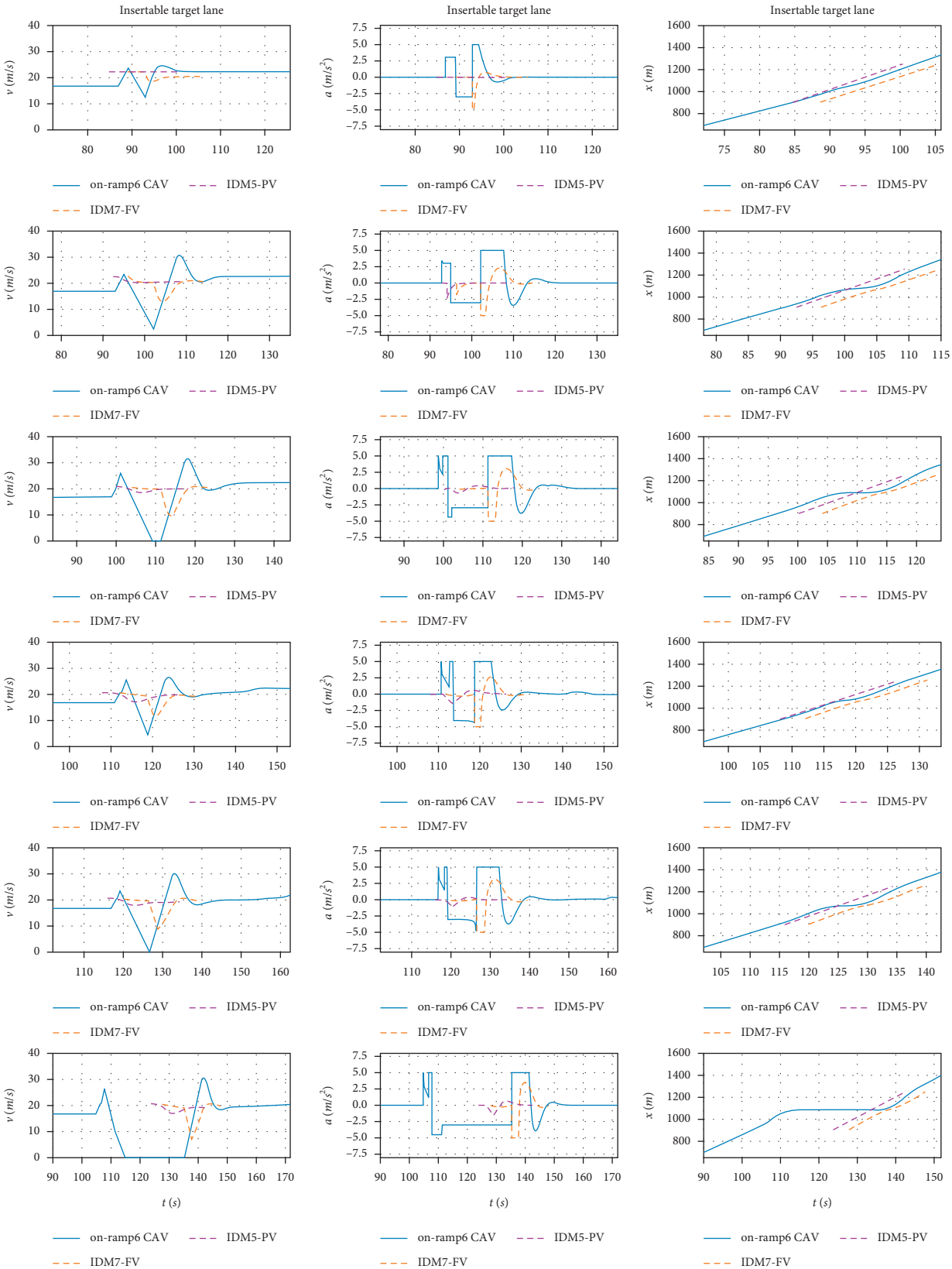

Figure 9: Data curve in "normal merging" without control.

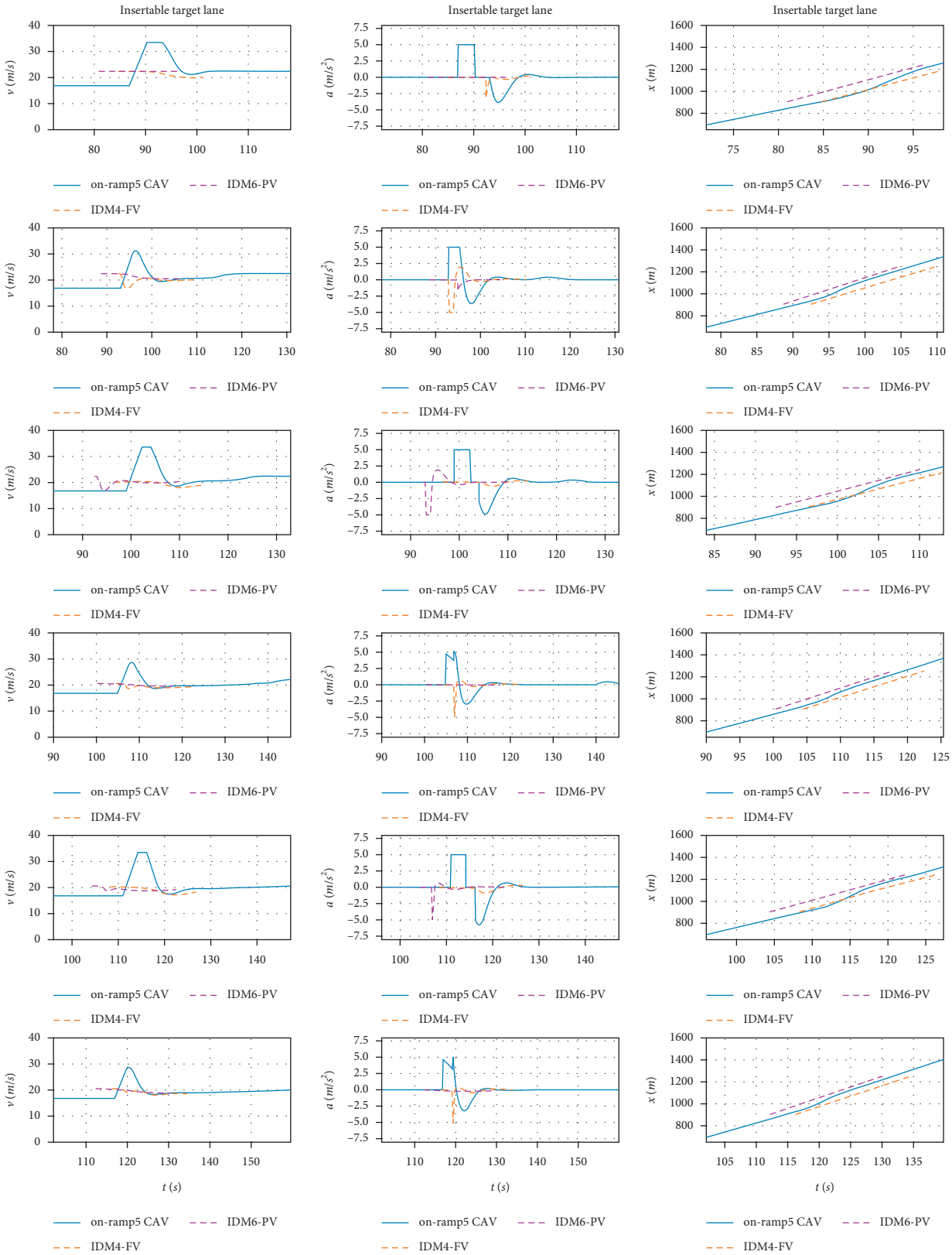

Figure 10: Data curve in the "proposed model" with control.

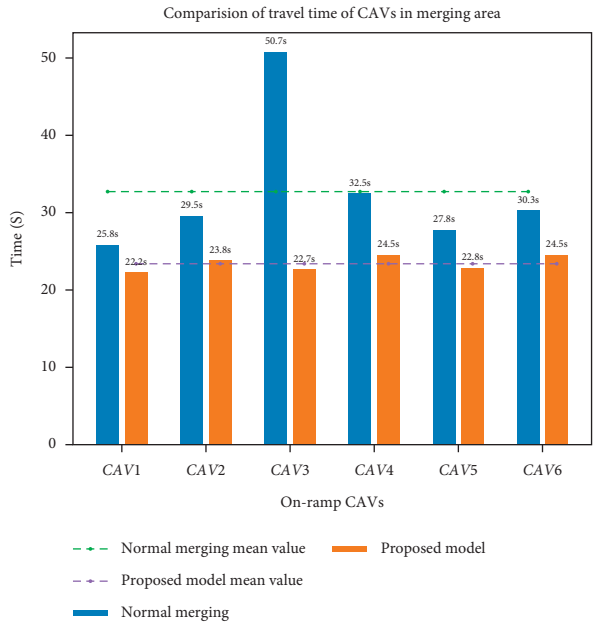

FIGURE 11: Comparison of travel time of CAVs in the merging area.

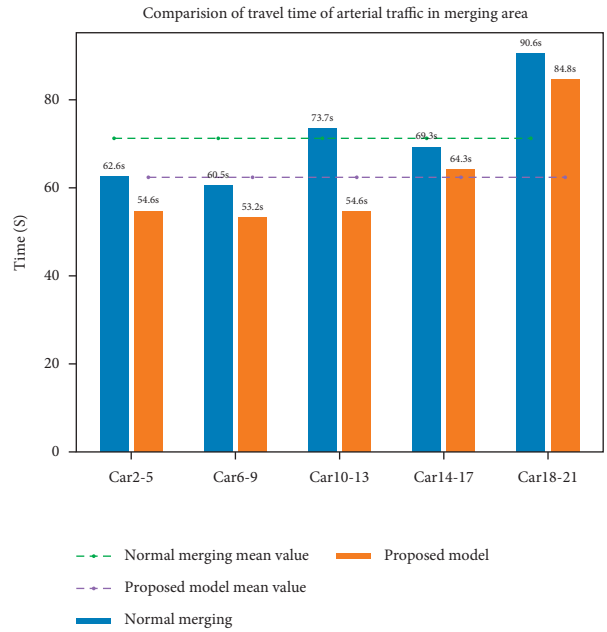

FIGURE 12: Comparison of travel time of arterial traffic in the merging area.

particles in the coordinate of the position curve are larger, so it is difficult to reflect small changes. Moreover, observing the acceleration curve (column 2), the acceleration changes frequently during the CAVs merging. This indicates that it is difficult for vehicles to cope with complex traffic dynamics on the arterial when merging, and frequent acceleration adjustment behaviors may lead to driving risks.

Conversely, it can be found that the amplitude and frequency of the acceleration curve are obviously reduced in Figure 10. It shows that the proposed model can effectively guarantee driving safety and make the merging process smoother. Surprisingly, unlike "normal merging", the parking wait time for CAV3 and CAV6 almost disappeared by observing the velocity curve (column 1) and the position curve (column 3). This means that the proposed model can coordinate with the dynamics of the arterial traffic flow, effectively plan the traveling control strategy, and improve the traveling efficiency of CAV merging. In addition, the acceleration curves of CAV4 and CAV6 show that when driving in the acceleration lane, the acceleration is adjusted, and a good merging effect is achieved, which explains the rationality of the design of situation 2-subsituation 2-Case 6 and situation 3-Case 8.

In order to visually show the efficiency improvement of the proposed model, we compared the travel time of 6 on-ramp CAVs from the beginning of the on-ramp to the completion of merging and exiting the merging area in "normal merging" and "proposed model," as shown in Figure 11. The CAV3 has the longest travel time of 50.7 s, but it changed to 22.7 s under control conditions, reducing travel time by 55%. In terms of the average travel time of the 6 CAVs, the "proposed model" is significantly lower than "normal merging." Based on the average value, the application of the proposed model resulted in a 28.7% reduction in CAV travel time. Moreover, the travel time of each CAV fluctuates within a very small range, approaching 23.4 s. This indicates that after featuring optimal merging positions, when the arterial traffic flows are randomly distributed, the time difference for merging is not much. That is, each CAV can approximately get a fair use of road resources.

As shown in Figure 12, a comparison of travel time of arterial traffic in the merging area is an aim to analyze the influence of the proposed model on surrounding traffic while assisting CAV merging. For the surrounding traffic, the travel time of all vehicles in the target lane (including the CAVs after merging) passing through the merging area was counted, and each vehicle was counted in a group of 4 until the last CAV left the merging area. The observation shows that the total travel time of each group in the "proposed model" is lower than that in "normal merging," which indicates that the proposed model does not sacrifice the interests of surrounding traffic to assist CAV merging. The group (car 10–13) with the greatest difference saw a 26% reduction in travel time after applying the proposed model.

5. Conclusion and Future Work

This work combines safety and coordination and assists CAVs merging with featuring optimal merging positions. Based on the traffic simulation experiment and discussion, the following conclusions can be drawn:

(1) The proposed model can effectively guarantee driving safety and make the merging process smoother by comparing the differences of data curves before and after the application of the proposed model

(2) The application of the proposed model resulted in a 28.7% reduction in travel time for the CAV merging

(3) The proposed model does not sacrifice the interests of surrounding traffic to assist CAV merging based

on the comparison of travel time of arterial traffic in the merging area

However, this work still has some limitations and several future research directions can be considered:

(1) We only study one vehicle type in arterial traffic, namely, human-driven vehicle. The arterial traffic can be set to mixed traffic flow (human-driven vehicle and CAVs) [36, 37]. Then, how to adapt the proposed model to the new environment must be considered.

(2) All merged CAVs are independent individuals. Subsequent studies can consider how to determine the optimal merging positions and driving strategy for the CAV platoon [38, 39].

(3) When the CAV merges, there is no obstacle in the acceleration lane. Future research can consider how to dynamically determine the optimal merging position when there are obstacle vehicles in the acceleration lane.

Data Availability

The data used to support the findings of this study are included within the article.

Conflicts of Interest

The authors declare that they have no conflicts of interest.

Acknowledgments

The paper received the research funding support from the Central Public-Interest Scientific Institution Basal Research Fund (2021-9081 and 2020-9018) and the Sichuan Science and Technology Program (2021YJ0535 and 2022YFG0152).

References

[1] S. Ahn, J. Laval, and M. J. Cassidy, "Merging and diverging effects on freeway traffic oscillations: theory and observation," *Transportation Research Record Journal of the Transportation Research Board*, vol. 2188, no. 1, pp. 1–8, 2010.

[2] Z. Zheng, S. Ahn, and D. Chen, "Freeway traffic oscillations: m," *Transportation Research Part B: Methodological*, vol. 45, no. 9, pp. 1378–1388, 2011.

[3] X. Li, F. Peng, and Y. Ouyang, "Measurement and estimation of traffic oscillation properties," *Transportation Research Part B*, vol. 44, no. 1, 2009.

[4] X. Shi, L. I. Q. Wen, and L. I. Z. Tie, "Method of designing acceleration lane length in freeway interchange," *Journal of Henan University*, Natural Science, vol. 30, no. 4, pp. 17–20.

[5] Z. Li and L. Li, "Computational method of acceleration lane length in expressway merging area," *Journal of Southeast University*, Natural Science Edition, vol. 46, no. 4, pp. 888–892, 2016.

[6] Y. S. Ci, L. N. Wu, X. Z. Ling, and Y. L. Pei, ""Operation reliability for on-ramp junction of urban freeway," *Journal of Central South University of Technology*, vol. 18, no. 1, pp. 266–270, 2011.

[7] Y. Wang and M. Papageorgiou, "Local ramp metering in the case of distant downstream bottlenecks," in *Proceedings of the Intelligent Transportation Systems Conference*, Toronto, Ontario, Canada, September 2006.

[8] M. Papageorgiou, "Overview of traffic signal operation policies for ramp metering," *Transportation Research Record*, vol. 2047, no. 1, pp. 28–36, 2008.

[9] R. C. Carlson, I. Papamichail, M. Papageorgiou, and A. Messmer, "Optimal motorway traffic flow control involving variable speed limits and ramp metering," *Transportation Science*, vol. 44, no. 2, pp. 238–253, 2010.

[10] N. Lu, N. Cheng, and N. Zhang, X. Shen, W. Jon, Mark. Connected vehicles: solutions and challenges," *IEEE Internet of Things Journal*, vol. 1, no. 4, 2014.

[11] P. Liu, C. Wang, and T. fu, "Yue ding exploiting opportunistic coding in throwbox-based multicast in vehicular delay tolerant networks," *IEEE Access*, vol. 7, 2019.

[12] Y. Gao, X. Xu, Y. L. Guan, and P. H. J. Chong, "V2X content distribution based on batched network coding with distributed scheduling," *IEEE Access*, vol. 6, 2018.

[13] G. Christine, S. R. Simon, and S. Annegret, "Vehicle-to-X (V2X) implementation: an overview of predominate trial configurations and technical, social and regulatory challenges. Renewable and Sustainable Energy Reviews," vol. 145, 2021.

[14] R. Scarinci and B. Heydecker, "Control concepts for facilitating motorway on-ramp merging using intelligent vehicles," *Transport Reviews*, no. 6, p. 34, 2014.

[15] R. T. Jackeline, M. A. Andreas, Automated and cooperative vehicle merging at highway on-ramps," *IEEE Transactions on Intelligent Transportation Systems*, vol. 18, no. 4, 2017.

[16] R. Pueboobpaphan, F. Liu, and B. V. Arem, "The impacts of a communication based merging assistant on traffic flows of manual and equipped vehicles at an on-ramp using traffic flow simulation," in *Proceedings of the Inter-national IEEE Conference on Intelligent Transportation Systems*, IEEE, Funchal, Portugal, September 2010.

[17] M. Dan, B. M. Jan Čurn, B. Mélanie, and C. Vinny, "On-ramp traffic merging using cooperative intelligent vehicles: a slot-based approach," in *Proceedings of the International IEEE Conference on Intelligent Transportation Systems*, IEEE, Anchorage, AK, USA, September 2012.

[18] J. Rios-Torres, A. Malikopoulos, and P. Pisu, "Online optimal control of connected vehicles for efficient traffic flow at merging roads," *IEEE 18th International Conference on Intelligent Transportation Systems*, 2015.

[19] H. Min, Y. Fang, X. Wu, G. Wu, and X. Zhao, "On-ramp merging strategy for connected and automated vehicles based on complete information static game," *Journal of Traffic and Transportation Engineering (English Edition)*, vol. 8, no. 4, pp. 582–595, 2021.

[20] W. Cao and M. Mukai, T. Kawabe, H. Nishira and F. Noriaki, . Cooperative vehicle path generation during merging using model predictive control with real-time optimization," *Control Engineering Practice*, vol. 34, pp. 98–105, 2015.

[21] J. Wang, F. Ma, Y. Yu et al., "Optimization design of the decentralized multi-vehicle cooperative controller for freeway ramp entrance," *International Journal of Automotive Technology*, vol. 22, no. 3, pp. 799–810, 2021.

[22] T. Zhixian and Z. Hong, Z. Xin, I. A. Miho, N. Hideki, A novel hierarchical cooperative merging control model of connected and automated vehicles featuring flexible merging positions in system optimization," *Transportation Research Part C*, vol. 138, 2022.

[23] C. Letter and L. Elefteriadou, "Efficient control of fully automated connected vehicles at freeway merge segments,"

Transportation Research Part C Emerging Technologies, vol. 80, no. 7, pp. 190–205, 2017.

[24] M. A. Chen, B. Ld, and A. Xz, "Event triggered rolling horizon based systematical trajectory planning for merging platoons at mainline-ramp intersection," *Transportation Research Part C: emerging Technologies*, vol. 125, 2021.

[25] W. Xiao, C. Belta, and G. C. Christos, *Decentralized Merging Control in Traffic Networks*, in *Proceedings of the 10th ACM/ IEEE International Conference on Cyber-Physical Systems*, Montreal Quebec Canada, April 2019.

[26] X. Qi and Fu Rui, "Ukkusuri Satish V., Yu Shaowei, Jiang Rui. Modeling and impact analysis of connected vehicle merging accounting for mainline random length tight-platoon," *Physica A: Statistical Mechanics and Its Applications*, vol. 563, 2021.

[27] Z. Gao and Z. Wu, H. Wei, K. Long, J. B. Young, K. Long, Optimal trajectory planning of connected and automated vehicles at on-ramp merging area," *IEEE transactions on intelligent transportation systems*, vol. 23, no. 8, 2021.

[28] L. C. Davis, "Optimal merging into a high-speed lane dedicated to connected autonomous vehicles," *Physica A: Statistical Mechanics and Its Applications*, vol. 555, Article ID 124743, 2020.

[29] Y. Yang, Z. Yuan, and R. Meng, "Exploring traffic crash occurrence mechanism toward cross-area freeways via an improved data mining approach," *Journal of Transportation Engineering Part A Systems*, vol. 148, no. 9, Article ID 04022052, 2022.

[30] W. J. Scholte, P. W. A. Zegelaar, and H. Nijmeijer, "A control strategy for merging a single vehicle into a platoon at highway on-ramps," *Transportation Research Part C*, vol. 136, 2022.

[31] C. Tianyi, "Wang Meng, Gong Siyuan, Zhou Yang, Ran Bin. Connected and automated vehicle distributed control for on-ramp merging scenario: a virtual rotation approach," *Transportation Research Part C*, vol. 133, 2021.

[32] Z. Sun, T. Huang, and P. Zhang, "Cooperative decision-making for mixed traffic: a ramp merging example," *Transportation Research Part C*, vol. 120, 2020.

[33] H. Jula, B. E. Kosmatopoulos, and P. A. Ioannou, "Collision avoidance analysis for lane changing and merging," *IEEE Transactions on Vehicular Technology*, vol. 49, no. 6, 2000.

[34] Y. Yang, N. Tian, Y. Wang, and Z. Yuan, "A parallel FP-growth mining algorithm with load balancing constraints for traffic crash data," *International Journal of Computers Communications & Control*, vol. 17, no. 4, p. 4806, 2022.

[35] A. Kanaris, B. E. Kosmatopoulos, and P. A. Ioannou, "Strategies and spacing requirements for lane changing and merging in automated highway systems," *IEEE Trans. Vehicular Technology*, vol. 50, 2001.

[36] Y. Jiang, S. Wang, Z. Yao, B. Zhao, and Y. Wang, "A cellular automata model for mixed traffic flow considering the driving behavior of connected automated vehicle platoons," *Physica A: Statistical Mechanics and Its Applications*, vol. 582, Article ID 126262, 2021.

[37] Z. Yao, Y. Jin, H. Jiang, L. Hu, and Y. Jiang, "CTM-based traffic signal optimization of mixed traffic flow with connected automated vehicles and human-driven vehicles," *Physica A: Statistical Mechanics and Its Applications*, vol. 603, Article ID 127708, 2022.

[38] Z. Yao, Q. Gu, Y. Jiang, and B. Ran, "Fundamental diagram and stability of mixed traffic flow considering platoon size and intensity of connected automated vehicles," *Physica A: Statistical Mechanics and its Applications*, vol. 604, 2022.

[39] Z. Yao, H. Jiang, Y. Cheng, Y. Jiang, and B. Ran, "Integrated schedule and trajectory optimization for connected automated vehicles in a conflict zone," *IEEE Transactions on Intelligent Transportation Systems*, vol. 23, no. 3, pp. 1841–1851, 2022.